Desalination and Water Treatment
www.deswater.com

doi: 10.5004/dwt.2017.0143

62 (2017) 108–119
February

Ultrafiltration of oil-in-water emulsion using a 0.04-μm silicon carbide membrane: Taguchi experimental design approach

Mohamed Zoubeik, Amr Henni*

Produced Water Treatment Laboratory, Faculty of Engineering and Applied Science, University of Regina, Saskatchewan S4S0A2, Canada, Email: amr.henni@uregina.ca (A. Henni), zoubeikm@uregina.ca (M. Zoubeik)

Received 31 January 2016; Accepted 9 June 2016

ABSTRACT

Oily wastewater as a by-product of the oil industry is becoming a major environmental concern. Finding effective means of treating and recycling the produced water is a key solution for the sustainability of the industry. Filtration experiments were performed to evaluate the performance of a new silicon carbide (SiC) ultrafiltration (UF) membrane in the separation of heavy oil from its brine. The Taguchi experimental design allowed for the investigation and determination of the optimal hydrodynamic conditions including transmembrane pressure (TMP), cross-flow velocity (CFV), temperature, and pH on the permeate flux, and also on the fouling resistance. In addition, the operating parameter with the greatest contribution to the permeate flux behaviour was determined using a statistical analysis of variance. The optimal operating conditions were found to be at 50°C, at a TMP of 0.9 bar, at a CFV of 0.5 m/s, and at a pH of 7. The TMP was found to have the utmost contribution to the permeate flux. Rejection capacity was also examined, and the SiC UF membrane achieved over 96% oil rejection, and one of the highest steady permeate flux levels for a UF membrane among what is published in the literature. Furthermore, models were used to investigate the fouling mechanisms involved in UF treatment of oily water. The cake formation model was found to be the best model for the correlation of the permeate flux decline.

Keywords: Produced water; Ultrafiltration; Silicon carbide; Taguchi method

1. Introduction

Discharge of oily water into the environment is rapidly increasing every year as the oil industry expands. It is becoming increasingly important to find effective and efficient methods to treat oily wastewaters.

Treatment with chemical or biological methods has many drawbacks such as high cost, use of toxic chemicals, additional pollution, and large footprint [1]. As a result, the physical treatment process using membrane technology is deemed promising. Membrane treatment systems enjoy some advantages in the form of small area space requirement, no need for chemical addition to the treatment process, and a consistent effluent quality [1]. The main types of membrane treatment systems include ceramic and polymeric membranes. Ceramic membranes are attractive to the oil industry due to their chemical resistance to inorganic acids, bases, oxidants, and their high thermal stability and longevity [2].

The main disadvantage of membrane processes is their flux decline. A principal reason for the decline during the initial period of operation for a membrane separation process is fouling. Fouling can occur in two ways, either by cake formation or by adsorption [3]. While cake formation is a reversible phenomenon [3], adsorption of particles is usually irreversible and involves the adsorption of elements on the membrane surface or within the pore walls [3]. In certain situations, adsorption of foulants can be undone with the use of aggressive chemical cleaning [3]. Fouling is determined by three main parameters: characteristics of the feed and membrane, and operating conditions [3]. The operating parameters play a major role when it comes to determining the rate

* Corresponding author.

of membrane fouling, especially transmembrane pressure (TMP). In general, an increase in TMP leads to a faster cake layer formation and plugging of pores [3].

Many studies focused on creating an optimal model for the description and prediction of permeate flux decline with time. Modeling is also employed to better understand the dynamics of membrane fouling. The most commonly used model is Hermia's model.

Hermia developed four empirical models in 1982 to describe membrane fouling, and these models are based on the constant pressure filtration laws [4]. Hermia's models include: complete pore blocking model, cake filtration model, standard pore blocking model and the intermediate pore blocking model (Fig. 1). The equations for each model are shown in Table 1, where J and J_0 are the actual and initial permeate fluxes, respectively. *Ks*, *Ki*, *Kb*, and *Kc* are the standard pore blocking, intermediate pore blocking, complete pore blocking, and cake formation model constants, respectively [5].

Membrane filtration of oily wastewater can be challenging to optimize. The operational parameters that can influence the permeate flux include the TMP, cross-flow velocity (CFV), temperature, and pH. Finding the optimal level for each parameter can be a time-consuming procedure. This can be circumvented by using an experimental design based on a fractional factorial design such as the Taguchi method [6].

Table 1
Mechanisms described by Hermia's model

Representative equations	Fouling mechanism
$\mathrm{Ln}(J) = \mathrm{Ln}(Jo) - K_b t$	Complete pore blocking
$\frac{1}{j^{1/2}} = \frac{1}{jo^{1/2}} + K_s t$	Standard pore blocking
$\frac{1}{J} = \frac{1}{J_o} + K_i A t$	Intermediate pore blocking
$\frac{1}{J^2} = \frac{1}{J_o^2} + K_c t$	Cake filtration

The method allows the investigation of a system using a set of factors of varying levels that impact a specific response [5]. It allows for the experimental determination of optimal conditions for the process, to find the contribution of the individual parameters, and also estimate the response under optimal conditions [5, 7]. It is a fractional factorial design that uses an orthogonal array (OA) to investigate the contribution of various factors on a process using a minimum number of possible experiments [7, 8]. The OA serves to reduce the number of experiments performed, and is based on the number of control factors and their levels [9].

Some researchers have examined the effectiveness of the Taguchi method. For example, Milić et al. [7] also used the Taguchi method to investigate the optimum conditions of an ultrafiltration (UF) ceramic membrane. The optimum conditions were found to be as follows: TMP = 5 bar, pH = 7 and an oil concentration = 0.5 v/v%; they showed the highest oil rejection to be 85%.

Abadi et al. [10] studied a microfiltration aluminum oxide ceramic membrane with a pore size of 0.2 μm for treating oily wastewater with an oil content of 26 mg/L, and obtained a Ttotal organic carbon (TOC) removal efficacy of over 95% and an oil removal of 85%. Vasanth et al. [11] fabricated low-cost microfiltration ceramic membranes composed of kaolin, quartz, calcium carbonate and titanium dioxide for treating oily water emulsions with an oil concentration of 100 mg/L and obtained an oil rejection of up to 94%. Alpatova et al. investigated the performance of a UF titanium dioxide/zirconium dioxide ceramic membrane for treating oil sands process-affected water and obtained a chemical oxygen demand (COD) removal up to 38.6% [2]. Another group investigated the use of modified ceramic UF membrane for oily water treatment and achieved an oil rejection rate of 88% [12]. Suresh et al. fabricated a membrane using fly ash and titanium and achieved high oil rejection rates of over 99% [13]. Zhu et al. also investigated the use of fly ash and titanium composite membrane for oily water treatment and achieved a TOC rejection of 97% [14]. Another group, Bayat et al. fabricated a multilayer UF aluminum-based membrane for oily water treatment and achieved an oil rejection rate of 84% [15]. Zsirai et al. investigated the use of UF silicon carbide membrane and achieved an average oil removal of 73% with high permeate flux rates [16].

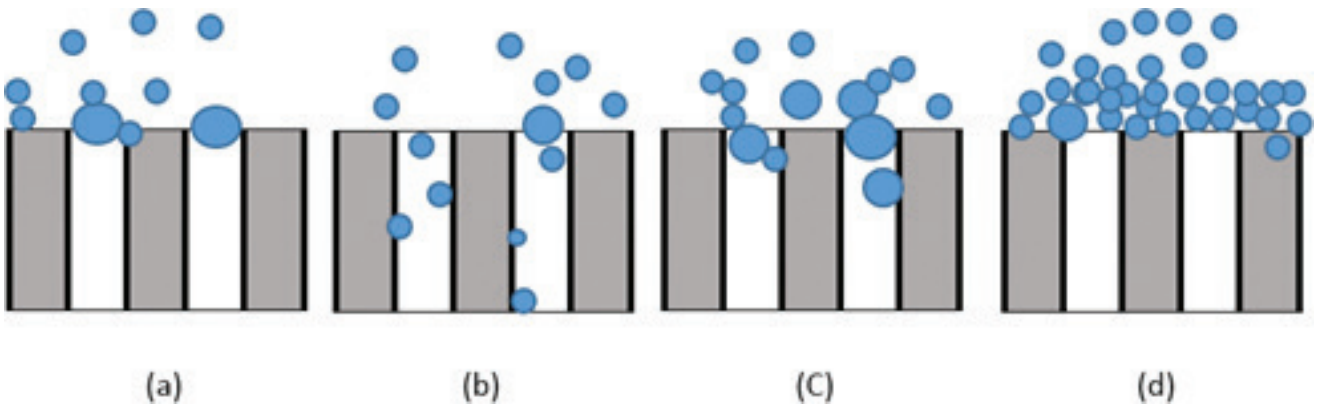

Fig. 1. Representation of different membrane fouling: (a) complete pore blocking, (b) standard blocking, (c) intermediate blocking, (d) cake layer formation.

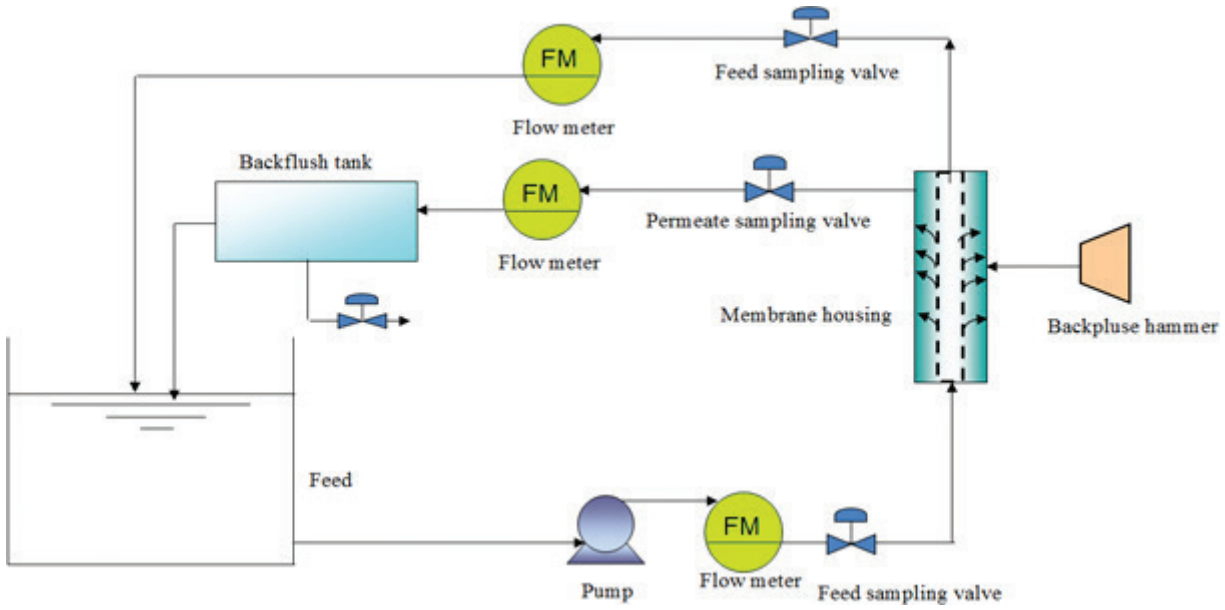

Fig. 2. P&ID of the LabBrain setup (adapted from [20]).

The majority of investigators have found that microfiltration ceramic membranes are effective for oil removal. However, in general, UF membranes are seen as one of the most effective treatment option for oily wastewater [17–19]. UF have higher oil rejection rates and lower operational costs, as reported by Bilstad and Espedal [19]. In a study, they compared UF and microfiltration and showed that UF was more efficient for meeting effluent standards for total hydrocarbons, suspended solids and dissolved compounds [19]. In addition, UF is effective for removal of heavy metals contrary to microfiltration membranes [17]. Nanofiltration is needed when the salt content in the oily water is high [17].

The present work describes the UF of oil in water emulsion using a new silicon carbide membrane. The Taguchi experimental design and subsequent analysis were used to elucidate the optimal hydrodynamic conditions and find the operating conditions with the greatest influence on permeate flux prediction. The separation performance of the membrane was investigated using the LaBrain filtration unit (Fig. 2) (LiqTech, Denmark). Finally, flux regeneration was investigated using different chemical cleaning reagents, and flux decline was modeled using Hermia's models.

2. Experimental methodology

2.1. General procedure

All experimental runs were performed in a batch mode using cross-flow operation. All operating conditions such as TMP, CFV, temperature, valve opening percentages, permeate flow rate, retentate flow rate, and feed flow rate were automatically logged every 3 s by the filtration setup. Each experimental run lasted about 1.5 h. For each experiment, about 24 L of oily emulsion were prepared. The characteristics of the prepared feed were tested for each experiment. The permeate characteristics were measured for each run for a variety of parameters. The parameters and the equipment used to measure them are listed in Table 2.

Table 2
Experimental equipment

Equipment	Function	Uncertainty	Manufacturer
Oil content analyzer – OCMA 350	Oil and grease content	4 mg/L	Horiba
TOC-LCPH Combustion Analyzer	Measures combustible heavy and light organic molecules	4 ug/L	Shimadzu
Mastersizer 3000 – Hydro LV	Droplet size	0.6%	Malvern
Zetasizer Nano – ZS	Zeta potential	0.12 μm	Malvern
HI 4522 – Total dissolved solids (TDS) meter	TDS and conductivity	0.01 ppm, μS/cm	Hanna
DR 5000 Spectrophotometer	Chemical oxygen demand (COD)	23 mg/L	Hach
HI 83414 – Turbidity & Free/Total Chlorine	Turbidity	2%	Hanna
HI 4521 & 4522 Bench Meters	pH	0.002	Hanna
Density Meter DSA 5000M	Density	0.000005 g/cm^3	Anton Paar
Viscometer DV-II +Pro	Viscosity	1.0%	Brookfield

Table 3
Salts used for feed water preparation

Type of salt	Weight in grams per 2 L of RO water	Source
Calcium chloride	2.68	Sigma-Aldrich
Magnesium chloride	1.76	Sigma-Aldrich
Sodium chloride	21.19	EMD Chemicals
Sodium bicarbonate	0.36	Sigma-Aldrich
Potassium chloride	0.62	Sigma-Aldrich
Sodium sulphate	0.45	Sigma-Aldrich

Table 4
Feed characteristics

Parameter		Average feed	SD
Oil content (mg/L)		120.80	11.66
TOC (mg/L)		70.33	4.03
Inorganic carbon (IC) (mg/L)		24.79	7.85
COD (mg/L)		1780	200
TDS (ppt)		11.69	0.31
Conductivity (mS/m)		21.10	0.88
Turbidity (NTU)		299	37.23
Salinity (%)		42	2.98
Zeta potential (mv)		– 17	4.60
Size distribution (μm)	Dv10	0.23	0.01
	Dv50	6.44	0.06
	Dv90	20.90	0.03

2.2. Feed preparation

The feed was prepared by dissolving the calculated amount of salts in a total volume of 2 L of reverse osmosis (RO) quality water, as presented in the following table. The oil used was light oil from Southern Saskatchewan Bakken area. At 22.5°C, its density was 0.87844 g/cc and its viscosity was 5.23 cp. A volume of 0.3 ml of oil was added to each 2 L batch. The 2 L mixture was then placed in a blender for 2 min to allow for the salts to dissolve and the oil to mix. The salts used are shown in Table 3. This process was repeated to make a total volume of 24 L for the process feed. Modifications of the feed to change its pH level were done with the addition of either NaOH or HCL. Titration to achieve a pH of 11 was achieved by adding 1 M NaOH, and that to achieve a pH of 5 was done by adding 1 M HCL. The pH was determined with a pH meter with an accuracy of 0.002. The feed mixture was heated to obtain the desired temperature (±1°C).

2.3. Membrane

The necessary information to fully describe the ceramic membrane used in this study is presented in Table 5, and a representation is shown in Fig. 3.

2.4. Cleaning procedure

Flux recovery using a variety of cleaning chemicals was investigated with the reagents listed in Table 6. The concentration used in the feed was attained by mixing the cleaning chemical with tap water to achieve the final concentration shown in Table 6. All cleaning chemicals were obtained from Fisher Scientific except for nitric acid which was purchased from BDH Chemicals. The same feed was used for all experiments with the characteristics outlined in Table 4, at a pH of 7, and at a temperature of 25°C. The RO flux was initially measured, and then measured again following feed filtration, after 1.5 h.

Table 5
Characteristics of ceramic membrane used in this experiment

Parameter	Description
Material	Silicon carbide (SiC)
Number of channels	1
Dimensions (mm)	25 ± 1 × 305 ± 1
Inside diameter (mm)	17
Outside diameter (mm)	25
Membrane area ($m^{2)}$	0.0163
pH range	0–14
Operating pressure (bar)	Max. 10 bar recommended below 3 bar
Maximum temperature (°C)	Determined by system components
Chlorine concentration	Unlimited
Cleaning	Chlorine, acid, caustic, solvent, oxidizers
Nominal pore size	0.04 μm

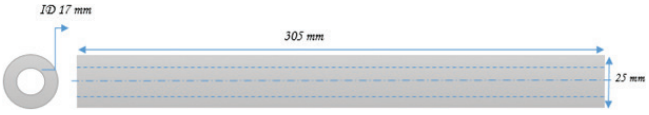

Fig. 3. Representation of ceramic membrane used in this experiment.

Table 6
List of cleaning solutions used in the experiment

Cleaning solutions	Concentration used in feed
KOH – Potassium hydroxide	4%
NaOH – Sodium hydroxide	4%
EDTA – Ethylenediaminetetraacetic acid	30 mM
SDS – Sodium dodecylsulphate	4 mM
H3PO4 – Phosphoric acid	2–4%
HNO3 – Nitric acid	4%

2.5. Experimental design based on Taguchi method

Using the Taguchi method of experimental design, four factors were adjusted, each, with three levels (low, medium and high). The experiment matrix was designed by selecting an appropriate OA (L9 array). Thus, the number of

Table 7
Parameters and their corresponding values based on their levels

Parameter	Designation	1	2	3
TMP (bar)	A	0.3	0.6	0.9
CFV (m/s)	B	0.5	1	1.5
Temp	C	30	40	50
pH	D	5	7	11

Table 8
Design of experiment for L9 array

Experimental run	A	B	C	D
1	1	1	1	1
2	1	2	2	2
3	1	3	3	3
4	2	1	2	3
5	2	2	3	1
6	2	3	1	2
7	3	1	3	2
8	3	2	1	3
9	3	3	2	1

Table 9
Values of parameters for each experimental run performed

TMP (bar)	CFV (m/s)	Temp	pH
0.3	0.5	30	5
0.3	1.0	40	7
0.3	1.5	50	11
0.6	0.5	40	11
0.6	1.0	50	5
0.6	1.5	30	7
0.9	0.5	50	7
0.9	1.0	30	11
0.9	1.5	40	5

experiments needed to examine the important effects can be condensed to 9, whereas full factorial experimentation requires $3^3 = 27$ experiments. The three levels of L9 OA are shown in Table 7. They were used for the optimization process and corresponding flux and fouling resistance were obtained at the nine selected conditions for each run as shown in Tables 8 and 9. Analysis of variance (ANOVA) was applied to determine the significance of each factor.

3. Results and discussions

3.1. Flux decline phenomenon

Fig. 4 shows changes in flux over time for each experimental run performed in this study. It displays an initially pronounced flux decline early in the filtration process before reaching a steady state where the flux decline plateaus. The reduction rate of permeate flux becomes much slower after about 30 min of filtration. The highest permeate flux is

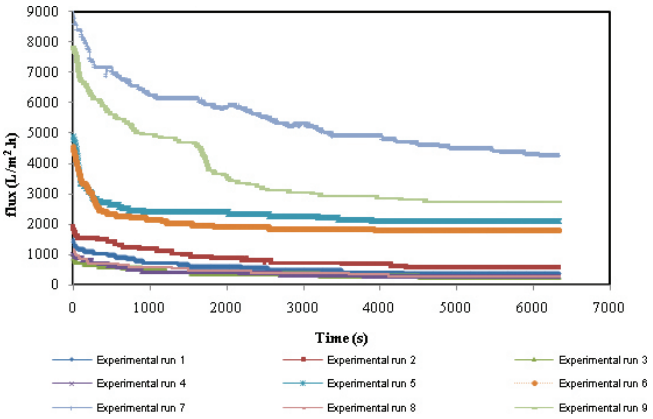

Fig. 4. Permeate flux decline as function of time.

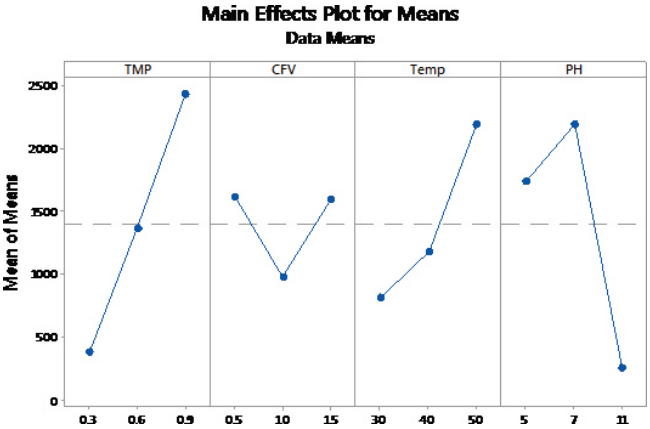

Fig. 5. Influence of individual process parameters on permeate flux (L/m² h) at different levels.

seen in experimental run 7 and the lowest in experimental run 3. This corresponds to an increase in TMP that leads to an increase in the permeate flux due to an increasing driving force [21]. Overall, the permeate flux for this silicon carbide membrane is much higher than typical ceramic membranes found in the literature [2, 12, 22].

3.2. Taguchi method analysis

Results obtained in implementing the Taguchi method analysis allowed for the generation of a graph presented in Fig. 5. The figure also shows the main effects on the permeate flux and shows the hydrodynamic factor with the greatest contribution to the flux as a function represented by the slope of the lines. The graph with the steepest slope represents the factor with the greatest contribution [7]. Accordingly, the TMP has the strongest influence on permeate flux followed by pH and temperature. The nonlinear distribution of pH and CFV is a reflection of the potential bilateral effect of these parameters on the permeate flux [21].

In addition, the Taguchi method analysis was used to obtain a signal-to-noise (SN) ratio for each experimental run performed, as presented in Table 10. The larger the better criteria was selected in the analysis as our aim was to achieve the largest permeate flux, and thus the operating parameters that maximize the SN ratio would

be the optimum operating conditions. Higher values of SN identify control factor settings that minimize the effects of the noise factors which are usually uncontrollable factors in the product used, but are controlled with our experimentation. As seen in Table 10, run 7 has the largest SN ratio and thus the optimum operating parameters are as follows: TMP of 0.9 bar, CFV of 0.5 m/s, Temp of 50°C and pH of 7.

The SN ratio is based on the following calculation [23]:

$$SN = -10\log\left(\frac{1}{n}\Sigma 1/y_i^2\right) \quad (1)$$

The interaction plot, shown in Fig. 6, allows for the examination of possible interaction effects seen as a change in the simple main effect of one variable over levels of a second variable. For example, the first row of graphs, reading from left to right, tells if changes in TMP are affected by the different levels of CFV, temperature and pH. The first graph indicates an interaction of CFV and TMP. The permeate flux is higher when operating at a TMP of 0.9 at CFV of 0.5 and 1.5. However, when the CFV is 1 m/s, the flux drops below what is seen for TMP of 0.3 and 0.9 bar. The flux is stable when operating at a low TMP of 0.3 across all levels of CFV.

The next graph looks at the interaction between temperature and TMP. The flux remains stable with very little fluctuations when operating at a low TMP of 0.3 across all temperatures. However, a higher flux is achieved when operating at 0.6 bar at high and low temperatures only. The flux has a linear relationship when the highest TMP is used where the flux continues to increase with increasing temperature. The last graph, in the first row, shows the interaction between pH and TMP. Due to minimal interaction between these two factors, the graphs are not overlapping.

In the next row of graphs, the plot of the interaction of CFV with temperature is presented. At lower temperatures, the highest flux is achieved with the highest CFV. However, at higher temperatures, the highest flux is achieved with the lowest CFV. The next graph shows the interaction of CFV with pH. It can be concluded that at low levels of CFV the flux is maximized at natural pH settings; however, the flux is minimized with acidic or basic feeds. The last graph shows plots of the interaction between pH and temperature. The flux is highest for acidic feeds with low or high temperature. However, at alkaline conditions, the temperature does not appear to affect the flux. The overall conclusion from the interaction plot is that the greatest interaction is seen between TMP and CFV.

To confirm the actual relative contribution of the process parameters and their effects, and to determine which factors have the most influence on permeate flux, an ANOVA statistical analysis was performed.

Table 10
SN ratios obtained using the Taguchi method

Trials	TMP (bar)	CFV (m/s)	Temp	pH	Flux L/m²·h	SN ratio
1	0.3	0.5	30	5	369	51.32
2	0.3	1.0	40	7	553	54.37
3	0.3	1.5	50	11	246	47.81
4	0.6	0.5	40	11	246	47.81
5	0.6	1.0	50	5	2088	66.39
6	0.6	1.5	30	7	1781	65.01
7	0.9	0.5	50	7	4238	72.54
8	0.9	1.0	30	11	307	49.75
9	0.9	1.5	40	5	2764	68.83

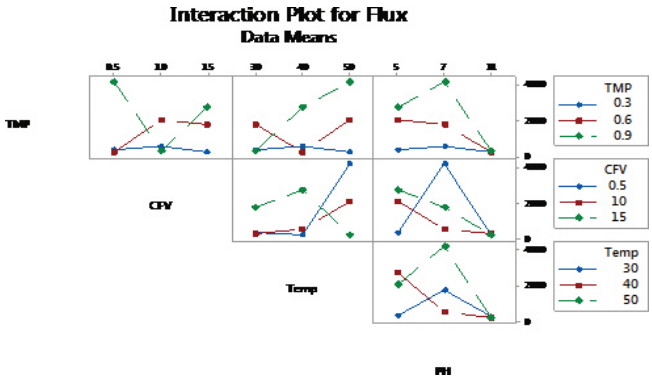

Fig. 6. Interaction plot for the flux (L/m² h).

3.3. ANOVA results

An ANOVA was performed in order to determine the statistical significance among the different factors. ANOVA evaluates the significance of the controlling factors by calculating the percentage of its contribution as shown in the figure below. The percentage contribution for each factor is defined as the portion of the total observed variance in the experiment for each significant factor. The greater the value, the more it contributes to the final result [9, 23]. The ANOVA results are shown in Fig. 7 and Table 11 where the last column contains the percentage contribution for each factor, showing TMP as the factor with the highest contribution. This confirms the results from the Taguchi experimental graph analysis which also shows that the TMP provides the strongest contribution to permeate flux control.

To allow for the completion of the ANOVA analysis, the parameter with the lowest contribution is removed in this work, and the operating parameter with the least influence on permeate flux was found to be CFV. The optimum conditions as determined by ANOVA are reflected in the F-ratio which provides another way to assess for the significance of the factors. The F-ratio is defined as the ratio of variance due to the effect of a special factor on the variance compared with the error term [24]. When the F-ratio is below 1, the contribution of the factor is minimal and is thus not a significant factor. As seen in Table 12, the factor with the lowest F-ratio is the CFV. When examining Table 12 with the pooled ANOVA results, TMP is the factor with the largest F-ratio, thereby confirming again that it is the factor with the greatest contribution to permeate flux determination of decline.

3.4. Effluent characteristics

The effectiveness of the UF process for oily emulsion was evaluated by examining the characteristics and the quality of the permeate. The next series of tables shows the characteristics of feed in comparison with the permeate characteristics,

Table 11
Analysis of variance (ANOVA) – OA L9

Factor	DOF	Sum of square	Mean of square	F-ratio	P (%)
TMP (bar)	2	6,291,055	3,145,527	1.56	38.90
CFV (m/s)	2	780,513	390,256	0.19	4.83
Temp	2	3,023,965	1,511,982	0.75	18.70
pH	2	6,079,788	3,039,894	1.50	37.59
Error	0	0	0		0
Total	8	16,175,322	2,021,915		100
Error	2	780,513	390,256		

Table 12
Final results of variance analysis (ANOVA) – OA L9

Factor	DOF	Sum of square	Mean of square	F-ratio
TMP (bar)	2	6,291,047	3,145,524	8.06
CFV (m/s)	2		Pooled	
Temp	2	3,023,956	1511978	3.87
pH	2	6,079,813	3039907	7.79
Error	2	780,502	390251	
Total	8	16,175,318		

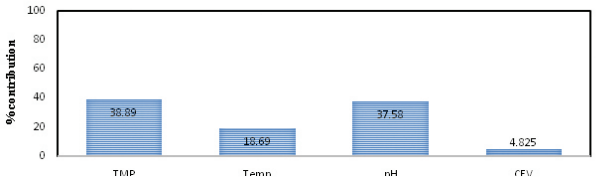

Fig. 7. Results of ANOVA for test series and effect of contribution of operating parameters (TMP, Temperature, pH and CFV) on flux.

and the rejection rates for a variety of parameters such as the oil content, TOC, inorganic carbon (IC), COD, total dissolved solids (TDS), conductivity, turbidity and salinity. From these results, it can be observed that the treatment efficiency is relatively high for certain parameters such as oil content, TOC, and turbidity where the rejection is above 95% as seen in Fig. S1 (Supplementary Information). However, the treatment efficiency for other parameters such as TDS and salinity is relatively low where the rejection is less than 10%. The operating parameters that achieved the highest oil content rejection of 96.7% are at a TMP of 0.3 bar and a CFV of 0.5 m/s.

3.5. Effects of operating parameters on flux and removal efficiencies

The overall experimental analysis shows that the TMP is responsible for the strongest contribution for permeate flux control followed by pH, Temp and CFV. Permeate flux increases with increasing TMP which is due to the increase in driving forces across the membrane [25]. However, with increasing TMP, fouling can occur at a faster rate when oil droplets become more compact on the membrane surface and block the pores [26]. Thus, at a certain TMP, permeate flux will no longer increase due to the formation of a fouling layer on the membrane [26]. In addition, removal efficiencies can be affected by increasing the TMP when the oil content removal efficacy dropped form 95% to 91% for an increase in TMP from 0.3 to 0.9 bar.

When examining the effect of CFV, this parameter was found to have the least effect on the permeate flux. As a general trend with an increase in CFV, the oil content removal efficiency decreases. At low CFV, the fouling layer develops easily leading to a decrease in filtration efficiency [27]. The fouling layer forms a filtration layer and restricts the passage of natural organic matter through the membrane, leading to an improvement in TOC removal [10]. Furthermore, at higher CFV rates, a boost in turbulence can enhance the permeate flux via increasing the shear stress and the reduction of the polarization concentration layer [28, 29]. This effect can be seen with increasing CFV; however, after a critical CFV value is reached, this effect is no longer significant [30].

Table 13
UF 0.04 μm permeate characteristics and rejection percentages at TMP 0.3 bar and CFV of 0.5, 1, and 1.5 m/s

TMP		0.5 m/s		1 m/s		1.5 m/s	
Parameter	Feed	Permeate	Rejection (%)	Permeate	Rejection (%)	Permeate	Rejection (%)
Oil content (mg/L)	120	4	96.67	6	95.01	9	92.51
TOC (mg/L)	77.70	2.9	96.27	2.3	97.04	2.1	97.29
IC (mg/L)	24.93	10.6	57.48	10.4	58.28	10.2	59.09
COD (mg/L)	1780	950	46.64	1005	43.56	980	44.96
TDS (ppt)	11.69	10.6	9.39	10.5	10.24	10.7	8.53
Conductivity (mS/m)	21.10	20	5.21	20.4	3.32	20.6	2.37
Turbidity (NTU)	298.90	0.5	99.85	0.25	99.93	0.3	99.91
Salinity (%)	42.1	38.1	9.61	39.0	7.47	40.0	5.10

Table 14
UF 0.04 μm permeate characteristics and rejection percentages at a TMP 0.6 bar and CFV of 0.5, 1, and 1.5 m/s

TMP		0.5 m/s		1 m/s		1.5 m/s	
Parameter	Feed	Permeate	Rejection (%)	Permeate	Rejection (%)	Permeate	Rejection (%)
Oil content (mg/L)	120	8	93.34	6	95.01	9	92.51
TOC (mg/L)	77.70	2.90	96.27	2.20	97.17	2.30	97.04
IC (mg/L)	24.93	10.80	56.68	11.00	55.88	11.10	55.48
COD (mg/L)	1780	970	45.52	950	46.64	1006	43.50
TDS (ppt)	11.69	10.90	6.82	10.40	11.10	10.80	7.68
Conductivity (mS/m)	21.10	20.00	5.21	20.40	3.32	20.60	2.37
Turbidity (NTU)	298.90	0.50	99.85	0.25	99.92	0.30	99.91
Salinity (%)	42.1	40.2	4.63	41.0	2.73	39.8	5.58

Table 15
UF 0.04 μm permeate characteristics and rejection percentages at TMP 0.9 bar and CFV of 0.5, 1, and 1.5 m/s

TMP		0.5 m/s		1 m/s		1.5 m/s	
Parameter	Feed	Permeate	Rejection (%)	Permeate	Rejection (%)	Permeate	Rejection (%)
Oil content (mg/L)	120	5	95.84	10	91.68	7	94.18
TOC (mg/L)	77.70	2.10	97.30	2.30	97.04	2.20	97.17
IC (mg/L)	24.93	10.70	57.08	10.90	56.28	10.50	57.88
COD (mg/L)	1780	1125	36.82	940	47.21	1110	37.66
TDS (ppt)	11.69	10.90	6.82	10.40	11.10	10.80	7.68
Conductivity (mS/m)	21.10	19.90	5.69	20.10	4.74	20.40	3.32
Turbidity (NTU)	298.90	0.50	99.85	0.25	99.93	0.30	99.91
Salinity (%)	42.1	40.0	5.10	40.2	4.63	38.9	7.71

The temperature of the feed can also affect the filtration function. As a general trend, when temperature increases, an increase in permeate flux occurs. It is known that increasing the temperature can decrease the viscosity of the feed and thus improve permeate flux [10]. In addition, as diffusivity increases, this contributes to the enhanced permeate flux [31]. However, the possible increase in flux must be balanced by the increase in operational costs involved with increasing the temperature.

Changing the pH of the feed has repercussions on the properties of the oily emulsion itself as well as the surface properties of the membrane [7]. The pH was the second most influential operating parameter contributing to permeate flux. The pH that achieved the highest flux was a pH of 7. It seems to have a bidirectional effect on permeate flux where natural pH seems optimum and a decrease in flux can be seen with acidic or alkaline conditions, more so with alkaline conditions. Variations of the feed pH can change the surface charge of the membrane resulting in a lower surface charge at acidic conditions. This can lead to changes in the electrostatic interactions between the charged particles in the feed and membrane's surface leading to alternation in the fouling process [8]. At alkaline conditions, electrostatic interactions increase at the membrane surface leading to changes to the membrane pore caliber which decreases the permeate flux [8]. As demonstrated in this experiment, the lowest steady state flux was achieved at a feed pH of 11. Summary of the experimental findings are seen in Tables 13–15.

Table 16
Correlation coefficient (R^2) values of Hermia's models

Experimental run	Standard pore blocking	Complete pore blocking	Intermediate pore blocking	Cake formation
Run 1	0.9308	0.8977	0.9506	0.9579
Run 2	0.9387	0.9113	0.955	0.9583
Run 3	0.9245	0.8911	0.9391	0.9337
Run 4	0.8898	0.7339	0.9108	0.9177
Run 5	0.6829	0.6288	0.7302	0.8043
Run 6	0.586	0.538	0.6302	0.7058
Run 7	0.9596	0.9408	0.9737	0.9898
Run 8	0.9315	0.9109	0.9399	0.9302
Run 9	0.8311	0.801	0.8542	0.8911

3.6. Prediction of permeate flux by Hermia's models

Table 16 reflects the fitting of experimental results to the Hermia's models. The correlation coefficient is used to assess which model has the best fit to the experimental results. It can be concluded that the cake formation model consistently

Table 17
Comparison between the experimental permeate flux and the permeate flux predicted by Hermia's models

Experimental run	Standard pore blocking	Complete pore blocking	Intermediate pore blocking	Cake formation	Measured (L/m²·h)
1	947	915	1,001	1,470	1,474
2	1,368	1,326	1,442	2,078	1,904
3	600	582	631	805	921
4	606	592	634	805	982
5	2,723	2,696	2,684	2,546	4,913
6	2,689	2,357	2,324	2,546	4,545
7	7,181	7,107	7,840	7,570	9,213
8	735	712	890	1,138	1,167
9	5,402	5,412	5,454	5,690	7,861

had higher R^2 values and is thus deemed the best fit to the model.

Table 17 compares the experimentally measured permeate flux values with the permeate flux values predicted by Hermia's models. For all experimental conditions, the difference between the measured and the predicted permeate flux values by (1) the standard pore blocking, (2) the complete pore blocking models, and (3) the intermediate pore blocking was more than 30%, while that by the cake filtration model was about 10%.

3.7. Critical flux determination

3.7.1. Comparison between filtrations at fixed TMP and fixed permeate flux

The critical flux in a membrane system is defined as the flux below which a decline of flux with time does not occur; however, above the critical flux, flux decline and fouling are observed [32]. The critical flux can be determined experimentally using two commonly used methods in the literature which include the flux-stepping method and the TMP stepping method. During the flux-stepping method, the permeate flux is controlled and incrementally increased while the TMP is allowed to rise and stabilize with each flux step [33]. The flux is raised slowly until an unsteady situation develops where the TMP rises rapidly with time indicating a rapid rise in fouling. The critical flux is thus defined as the lowest permeate flux at which this rapid rise in fouling starts to occur [32, 33].

On the other hand, the TMP stepping method allows to incrementally increase the TMP to permit the flux to rise and stabilize for each step. Once the flux increase becomes independent of the TMP, the critical flux is achieved. In this experimental work, both methods were used to determine the critical flux.

3.7.2. TMP stepping method

The variations of permeate flux with step increments of TMP were studied at CFV of 0.5, 1, and 1.5 m/s. The TMP was first set at 0.2 bar for 30 min to get a stabilized flux. The TMP was then increased by 0.2 bar increments every 30 min to allow for stabilization of the flux until the flux became pressure independent. The steady state flux achieved for each step of TMP was graphed vs. time with the corresponding TMP vs. time in the following graph (Fig. 8.).

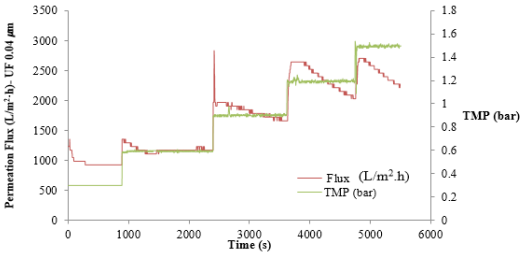

Fig. 8. Variations of permeate flux with time under step increments of transmembrane pressure at CFV of 0.5 m/s.

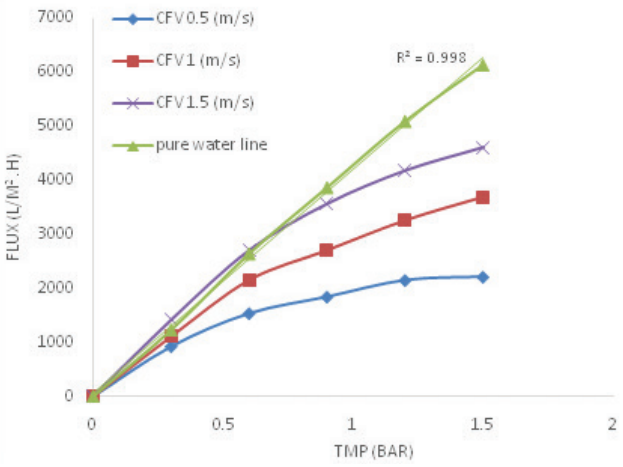

Fig. 9. Variation of stabilizsed permeate flux with TMP for different circulation velocities.

From the graph above, the critical flux is estimated to be between 2,500 and 2,800 L/m²·h as the flux seems to stabilize or plateau after a TMP of 0.8 bar.

For the first two TMP steps, the flux increases and then stabilizes; however, during further step increases, the flux reaches a peak and then decays to a plateau. A similar behavior was reported by Jaffrin et al. [34] who explained the decay after the peak to be due to the buildup of the concentration polarization adjusting itself to the new pressure.

The same experiment was repeated for different CFVs from 0.5 to 1.5 m/s. A summary graph is presented in Fig. 9. In the graph, the flux rises with TMP in a linear relationship independent of velocity until it reaches the critical flux where the permeate flux then levels off to a plateau; the height of each plateau corresponds to the critical flux achieved shown to increase linearly with velocity.

3.7.3. Flux-stepping method

The variations of TMP with step increments of flux were studied at CFV of 0.5, 1 and 1.5 m/s. The permeate flux was initially set to 10 L/m²·h and then 20, 30, 50, 70, 90, and 110 L/m²·h; this corresponds to about 613; 1,226; 1,840; 3,067; 4,294; 5,521 and 6,748 L/m²·h.

As shown by the graph below (Fig. 10), with each permeate flux step, TMP rises steadily and then stabilizes. However, once the critical flux is reached, the TMP rises more rapidly and does not stabilize, indicating rapid fouling. A steeper slope is seen after a flux of 2,500 L/m²·h is reached indicating that the critical flux at 0.5 m/s is around 2,500 L/m² h.

The same experiment was repeated for different CFVs from 0.5 to 1.5 m/s. The summary graph is seen in Fig. 11.

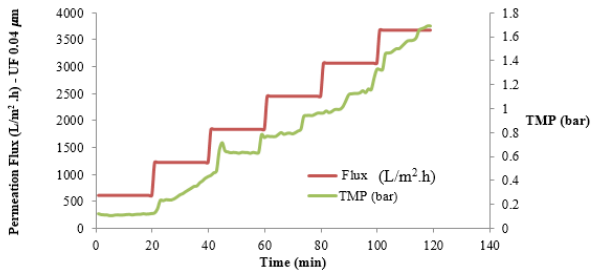

Fig. 10. Variations of TMP with time under step increments of permeate flux at CFV of 0.5 m/s.

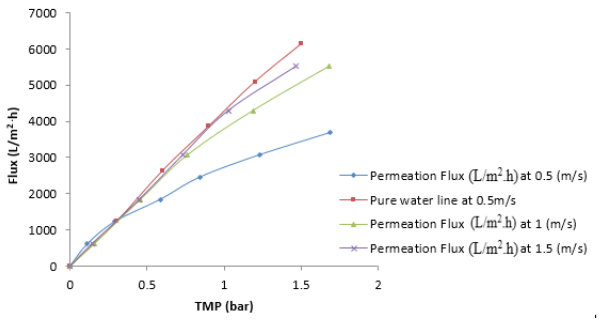

Fig. 11. Variation of stabilizsed permeate flux with TMP for different circulation velocities.

Using the flux-stepping method, the stabilized permeate flux and TMP relationship for different CFVs is graphed alongside the pure water line. The deviations from the pure water line signify the attainment of the critical flux. As the flux is increased, a cake layer begins to form on the surface of the membrane, and a deviation from the pure water line occurs [32]. As extrapolated from the graph below, the critical flux at CFV of 0.5 m/s is around 1,500 L/m²·h; at CFV of 1 m/s, it is 3,000 L/m²·h; and at CFV of 1.5 m/s, it is about 4,250 L/m²·h.

3.7.4. Comparison between tests at fixed permeate flux and fixed TMP

A comparison between both TMP stepping and the flux-stepping methods is presented in Fig. 12. In both cases, the flux and the TMP have stabilized values. When the graphs are superimposed onto each other, a value very close to the critical flux can be attained at low TMP readings; however, a small increase in flux can lead to a dramatic increase in TMP leading to an unstable scenario. The flux-stepping method is seen as a more accurate way to determine the critical flux when compared with the TMP stepping method since experiments that are carried out at a fixed flux where more likely to have a more stable TMP and that this method produced overall less fouling [33]. In addition, the TMP stepping method illustrates the concept of a limiting flux more so than a critical flux.

3.8. The effect of membrane cleaning on flux recovery

Membrane fouling is a major concern in produced water treatment. Thus, finding a cost effective and efficient method for cleaning the filtration membranes is essential. In this experimental work, different cleaning solutions and different combinations of these cleaning solutions were tested to find which is the most effective and which would achieve the highest flux recovery. The cleaning solutions used are summarized in Table 18. In general, three classes of cleaning solutions were used. Acidic cleaning solutions used included nitric and phosphoric acids which acted by hydrolysis of organic materials. Alkaline-based cleaning solutions used included potassium and sodium hydroxides. Alkaline-based solutions were chosen as they allow for the breakdown of proteins and organic materials and the saponification of oils [35]. Other cleaning solutions used were ethylenediaminetetraacetic acid (EDTA) as a metal

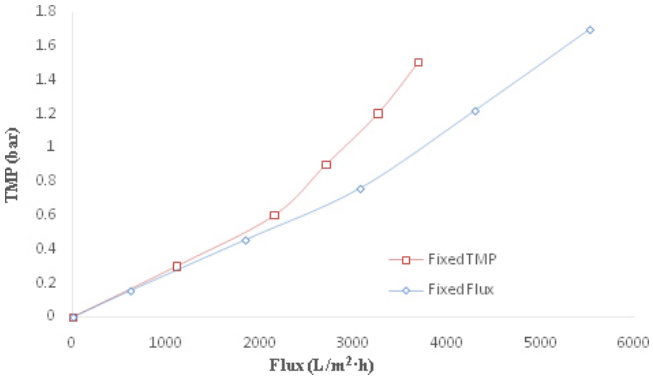

Fig. 12. Comparison between filtrations at fixed TMP and at fixed permeate flux.

Table 18
Membrane cleaning parameters and flux recovery

Chemical name	Time (min)	Concentration	Temperature (C°)	Initial RO flux (L/h)	RO flux – post-fouling (L/h)	RO Flux-post-cleaning (L/h)	Flux recovery (%)
$HNO_3 + H_3PO_4$	40	4% each	50	6,879	1,843	6,510	92.68
$HNO_3 + H_3PO_4$	30	4% each	50	6,879	1,904	6,449	91.46
KOH	30	4%	50	6,879	1,044	2,149	18.95
$KOH + HNO_3 + H_3PO_4$	30	4% each	50	6,879	1,044	6,818	98.95
EDTA	30	30 mM	50	6,879	1,843	6,142	85.00
EDTA + SDS	30	30 mM + 4 mM	50	6,879	1,965	6,142	85.91
H_3PO_4	30	4%	50	6,879	1,351	6,818	98.89
H_3PO_4	30	2%	50	6,879	1,965	6,204	86.25
NaOH	30	4%	50	6,879	2,088	4,484	50.00
$NaOH + HNO_3$	30	4% each	50	6,879	2,088	6,142	84.61
NaOH	30	4%	60	6,879	2,088	4,607	52.56
$NaOH + HNO_3$	30	4% each	60	6,879	2,088	6,449	91.03

chelating agent and sodium dodecylsulphate (SDS) as a surfactant. Surfactants are important because they can help in solubilizing and prevent re-deposition of foulants [35]. They also can modify the charge of the membrane surface. The following chemicals (NaOH, KOH, HNO_3, and H_3PO_4) were used as per recommendation of the membrane manufacturer, LiqTech. Based on the results, the best cleaning solutions used, in combination, were ($KOH+HNO_3+H_3PO_4$) which achieved a flux recovery of 98.95%. The worst cleaning agent was potassium hydroxide with only 18.95% flux recovery. In general, acidic cleaning solutions and the metal chelating agent were the most efficient achieving a flux recovery of over 98%. EDTA works by forming complexes with some particles, oil droplets and minerals, and separating them from the membrane surface [25]. Furthermore, when using a higher concentration of an acidic solution, the flux recovery was also higher as seen when comparing the two concentrations of phosphoric acid used.

4. Conclusion

The interaction effects of the operating parameters on the permeate flux decline, using a 0.04 -μm silicon carbide UF membrane, and its filtration capacity of synthetic oily water were experimentally tested. The UF membrane showed high efficiency of oil content removal and TOC rejection above 95%. The Taguchi methodology revealed that the TMP had the strongest contribution on permeate flux decline followed by pH and then temperature. The highest steady permeate flux was obtained at the following optimal conditions of temperature, TMP, CFV, and pH: 50°C, 0.9 bar, 0.5 m/s, and 7, respectively.

Hermia's models were used to compare the experimental results and predicted values of permeate flux. The results showed the best fitting model to the experimental data is the cake formation model followed by the intermediate pore blocking model for all experimental conditions tested.

Finally, the flux recovery was investigated using various cleaning solutions. Acidic solutions were found to have a higher efficacy where recovery rates of above 98% were achieved. The highest flux recovery was achieved with a mixture of cleaning solutions consisting of $KOH+HNO_3+H_3PO_4$.

Acknowledgement

The first author acknowledges the support of the FGSR at the University of Regina, CBIE (Canadian Bureau of International Education), and the Libyan government for the graduate scholarship.

Abbreviations

ANOVA — Analysis of variance
CFV — Cross-flow velocity
COD — Chemical oxygen demand
DOE — Design of experiments
EDTA — Ethylenediaminetetraacetic acid
IC — Inorganic carbon
FR — Flux recovery
F-ratio — A statistical value from ANOVA
P — Percentage contribution, %
NaOH — Sodium hydroxide
H_3PO_4 — Phosphoric acid
HNO_3 — Nitric acid
OA — Orthogonal array
SD — Standard deviation
SDS — Sodium dodecylsulphate
SN — Signal-to-noise
TMP — Transmembrane pressure
TOC — Total organic carbon
TDS — Total dissolved solids
UF — Ultrafiltration

References

[1] A. Fakhru'l-Razi, A. Pendashteh, L.C. Abdullah, D.R.A. Biak, S.S. Madaeni, Z.Z. Abidin, Review of technologies for oil and gas produced water treatment, J Hazard Mater., 170 (2009) 530–551.

[2] A. Alpatova, E.S. Kim, S. Dong, N. Sun, P. Chelme-Ayala, M.G. El-Din, Treatment of oil sands process-affected water with ceramic ultrafiltration membrane: effects of operating conditions on membrane performance, Sep Purif. Technol., 122 (2014) 170–182.
[3] L.Y. Ng, A.W. Mohammad, C.P. Leo, N. Hilal, Polymeric membranes incorporated with metal/metal oxide nanoparticles: a comprehensive review, Desalination, 308 (2013) 15–33.
[4] J. Hermia, Constant pressure blocking filtration laws—application to power-law non-newtonian fluids, Trans. Inst. Chem. Eng., 60 (1982) 183–187.
[5] A. Reyhani, K. Sepehrinia, S.M. Seyed Shahabadi, F. Rekabdar, A. Gheshlaghi, Optimization of operating conditions in ultrafiltration process for produced water treatment via Taguchi methodology, Desal. Wat. Treat., 54 (2015) 2669–2680.
[6] D. Allende, D. Pando, M. Matos, C.E. Carleos, C. Pazos, J.M. Benito, Optimization of a membrane hybrid process for oil-in-water emulsions treatment using Taguchi experimental design, Desal. Wat. Treat., 57 (2015) 1–10.
[7] J.K. Milić, I. Petrinić, A. Goršek, M. Simonič, Ultrafiltration of oil-in-water emulsion by using ceramic membrane: Taguchi experimental design approach, Cent. Eur. J. Chem., 12 (2014) 242–249.
[8] Z.B. Gönder, Y. Kaya, I. Vergili, H. Barlas, Optimization of filtration conditions for CIP wastewater treatment by nanofiltration process using Taguchi approach, Sep. Purif. Technol., 70 (2010) 265–273.
[9] A. Zirehpour, A. Rahimpour, M. Jahanshahi, M. Peyravi, Mixed matrix membrane application for olive oil wastewater treatment: process optimization based on Taguchi design method, J. Environ. Manage., 132 (2014) 113–120.
[10] S.R.H. Abadi, M.R. Sebzari, M. Hemati, F. Rekabdar, T. Mohammadi, Ceramic membrane performance in microfiltration of oily wastewater, Desalination, 265 (2011) 222–228.
[11] D. Vasanth, G. Pugazhenthi, R. Uppaluri, Cross-flow microfiltration of oil-in-water emulsions using low cost ceramic membranes, Desalination, 320 (2013) 86–95.
[12] S.E. Weschenfelder, A.M. Louvisse, C.P. Borges, E. Meabe, J. Izquierdo, J.C. Campos, Evaluation of ceramic membranes for oilfield produced water treatment aiming reinjection in offshore units, J. Petrol. Sci. Eng., 131 (2015) 51–57.
[13] K. Suresh, G. Pugazhenthi, Development of ceramic membranes from low-cost clays for the separation of oil–water emulsion, Desal. Wat. Treat., 57 (2016) 1927–1939.
[14] L. Zhu, M. Chen, Y. Dong, C.Y. Tang, A. Huang, L. Li, A low-cost mullite-titania composite ceramic hollow fiber microfiltration membrane for highly efficient separation of oil-in-water emulsion, Water Res., 90 (2016) 277–285.
[15] A. Bayat, H.R. Mahdavi, M. Kazemimoghaddam, T. Mohammadi, Preparation and characterization of γ-alumina ceramic ultrafiltration membranes for pretreatment of oily wastewater, Desal. Wat. Treat., (2016) 1–11.
[16] T. Zsirai, A.K. Al-Jaml, H. Qiblawey, M. Al-Marri, A. Ahmed, S. Bach, S. Watson, S. Judd, Ceramic membrane filtration of produced water: impact of membrane module, Sep. Purif. Technol., 165 (2016) 214–221.
[17] M. Padaki, R. Surya Murali, M.S. Abdullah, N. Misdan, A. Moslehyani, M.A. Kassim, Nidal Hilal, A.F. Ismail, Membrane technology enhancement in oil–water separation: a review, Desalination, 357 (2015) 197–207.
[18] Y. He, Z.W. Jiang, Technology review: treating oilfield wastewater, Filtration and Separation, 45 (2008) 14–16.
[19] T. Bilstad, E. Espedal, Membrane separation of produced water, Water Sci. Technol., 34 (1996) 239–246.
[20] LiqTech, User manual for LabBrain CFU025. (2013) Ballerup, Denmark.
[21] A. Salahi, M. Abbasi, T. Mohammadi, Permeate flux decline during UF of oily wastewater: experimental and modeling, Desalination, 251 (2010) 153–160.
[22] M. Ebrahimi, D. Willershausen, K.S. Ashaghi, L. Engel, L. Placido, P. Mund, P. Bolduan, P. Czermak, Investigations on the use of different ceramic membranes for efficient oil-field produced water treatment, Desalination, 250 (2010) 991–996.
[23] A. Ezzati, E. Gorouhi, T. Mohammadi, Separation of water in oil emulsions using microfiltration, Desalination, 185 (2005) 371–382.
[24] M. Hesampour, A. Krzyzaniak, M. Nyström, Treatment of waste water from metal working by ultrafiltration, considering the effects of operating conditions, Desalination, 222 (2008) 212–221.
[25] A. Salahi, T. Mohammadi, Experimental investigation of oily wastewater treatment using combined membrane systems, Water Sci. Technol., 62 (2010) 245–255.
[26] R. Ghidossi, D. Veyret, J.L. Scotto, T. Jalabert, P. Moulin, Ferry oily wastewater treatment, Sep. Purif. Technol., 64 (2009) 296–303.
[27] F.L. Hua, Y.F. Tsang, Y.J. Wang, S.Y. Chan, H. Chua, S.N. Sin, Performance study of ceramic microfiltration membrane for oily wastewater treatment, Chem. Eng. J., 128 (2007) 169–175.
[28] M. Hesampour, A. Krzyzaniak, M. Nyström, The influence of different factors on the stability and ultrafiltration of emulsified oil in water, J. Membrane Sci., 325 (2008) 199–208.
[29] S.S. Madaeni, M.K. Yeganeh, Microfiltration of emulsified oil wastewater, J. Porous Mater., 10 (2003) 131–138.
[30] T. Mohammadi, A. Esmaeelifar, Wastewater treatment of a vegetable oil factory by a hybrid ultrafiltration-activated carbon process, J. Membrane Sci., 254 (2005) 129–137.
[31] M. Abbasi, M. Mirfendereski, M. Nikbakht, M. Golshenas, T. Mohammadi, Performance study of mullite and mullite–alumina ceramic MF membranes for oily wastewaters treatment, Desalination, 259 (2010) 169–178.
[32] H. Falahati, A.Y. Tremblay, Flux dependent oil permeation in the ultrafiltration of highly concentrated and unstable oil-in-water emulsions, J. Membrane Sci., 371 (2011) 239–247.
[33] L. Defrance, M.Y. Jaffrin, Comparison between filtrations at fixed transmembrane pressure and fixed permeate flux: application to a membrane bioreactor used for wastewater treatment, J. Membrane Sci., 152 (1999) 203–210.
[34] M.Y. Jaffrin, L.H. Ding, M. Defossez, J.M. Laurent, Interpretation of transient ultrafiltration and microfiltration of blood and protein solutions, Chem. Eng. Sci., 50 (1995) 907–915.
[35] A. Trentin, C. Güell, T. Gelaw, S. De Lamo, M. Ferrando, Cleaning protocols for organic microfiltration membranes used in premix membrane emulsification, Sep. Purif. Technol., 88 (2012) 70–78.